



National Environmental  
Research Program

TROPICAL ECOSYSTEMS *hub*

Technical Report

## The relationship between Burdekin River discharges and photic depth in the central Great Barrier Reef



Murray Logan, Katharina Fabricius, Scarla Weeks, Marites Canto,  
Sam Noonan, Eric Wolanski and Jon Brodie



Australian Government

Department of Sustainability, Environment,  
Water, Population and Communities



# **The relationship between Burdekin River discharges and photic depth in the central Great Barrier Reef**

Murray Logan<sup>1</sup>, Katharina Fabricius<sup>1,\*</sup>, Scarla Weeks<sup>2</sup>, Marites Canto<sup>2</sup>  
Sam Noonan<sup>1</sup>, Eric Wolanski<sup>3</sup> and Jon Brodie<sup>3</sup>

<sup>1</sup> Australian Institute of Marine Science, PMB No 3, Townsville, Queensland 4810, Australia

<sup>2</sup> Biophysical Oceanography Group, School of Geography, Planning and Environmental Management,  
University of Queensland

<sup>3</sup> TropWATER, James Cook University, Townsville

\* Corresponding author: k.fabricius@aims.gov.au, phone: +61 7 47534412, fax: +61 7 47725852

Key words: Water clarity, remote sensing, transparency, turbidity, suspended particulate matter, river discharge, rainfall, Burdekin River, Queensland, Australia



**Australian Government**

---

**Department of Sustainability, Environment,  
Water, Population and Communities**

Supported by the Australian Government's National Environmental Research Program  
Project 4.1: Tracking coastal turbidity over time and demonstrating the effects of river discharge events  
on regional turbidity in the GBR

© Australian Institute of Marine Science (AIMS)

National Library of Australia Cataloguing-in-Publication entry:

978-1-921359-80-4

This report should be cited as:

Murray Logan, Katharina Fabricius, Scarla Weeks, Marites Canto, Sam Noonan, Eric Wolanski and Jon Brodie (2013) The relationship between Burdekin River discharges and photic depth in the central Great Barrier Reef. Report to the National Environmental Research Program. Reef and Rainforest Research Centre Limited, Cairns (29pp.).

Published by the Reef and Rainforest Research Centre on behalf of the Australian Government's National Environmental Research Program (NERP) Tropical Ecosystems (TE) Hub.

The Tropical Ecosystems Hub is part of the Australian Government's National Environmental Research Program. The NERP TE Hub is administered in North Queensland by the Reef and Rainforest Research Centre Limited (RRRC). The NERP Tropical Ecosystems Hub addresses issues of concern for the management, conservation and sustainable use of the World Heritage listed Great Barrier Reef (GBR) and its catchments, tropical rainforests including the Wet Tropics World Heritage Area (WTWHA), and the terrestrial and marine assets underpinning resilient communities in the Torres Strait, through the generation and transfer of world-class research and shared knowledge.

This publication is copyright. The Copyright Act 1968 permits fair dealing for study, research, information or educational purposes subject to inclusion of a sufficient acknowledgement of the source.

The views and opinions expressed in this publication are those of the authors and do not necessarily reflect those of the Australian Government or the Minister for Sustainability, Environment, Water, Population and Communities.

While reasonable effort has been made to ensure that the contents of this publication are factually correct, the Commonwealth does not accept responsibility for the accuracy or completeness of the contents, and shall not be liable for any loss or damage that may be occasioned directly or indirectly through the use of, or reliance on, the contents of this publication.

Cover photograph: MODIS-Aqua Quasi-True Colour Image of the Burdekin Region, from 23 October 2008.

This report is available for download from the NERP Tropical Ecosystems Hub website:

<http://www.nerptropical.edu.au/research>

01 June 2013

# Contents

Contents.....	i
List of Figures.....	ii
List of Tables.....	iii
Acknowledgements .....	iii
Summary .....	1
Introduction .....	2
Methods .....	6
MODIS data: Photic depth .....	6
Environmental data.....	8
Statistical analyses .....	8
Results .....	12
Spatial and seasonal patterns in photic depth .....	12
Relationship of photic depth to environmental drivers: Lag effects .....	14
Relationship of photic depth to environmental drivers: Changes in annual mean photic depth (averaged across the whole Burdekin region) .....	15
Relationship of photic depth to environmental drivers: Changes in daily mean photic depth (averaged across the whole Burdekin region) .....	17
Seasonal decomposition: Inter-annual patterns .....	18
Seasonal decomposition: Intra-annual patterns .....	21
References .....	27

## List of Figures

Figure 1: MODIS-Aqua Image of the Burdekin Region during a moderate flood discharge event (10 <sup>th</sup> February 2007). Image provided by NASA and processed by Matt Slivkoff. ....	3
Figure 2: Map of the Great Barrier Reef, with the Secchi data stations used for calibration marked as red crosses. ....	7
Figure 3: The spatial extent of the Burdekin Region, and an example of spatial patterns in photic depth within the Burdekin NRM Region. The colour contours indicate mean photic depth for September. ....	7
Figure 4: The five transects across the shelf (coastal: 0-0.1 across, inner: 0.1-0.25 across, lagoon: 0.25-0.45 across, midshelf: 0.45-0.65 across, outer shelf: >0.65 across). ....	9
Figure 5: Time series traces of daily trends in region-wide water clarity, and climatic and river variables. ....	13
Figure 6: Cross-correlation lags for daily water clarity against various environmental drivers a) Wave height (m), b) Wave frequency, c) Tidal range (m), d) Rainfall (mm) and e) Burdekin River discharge ....	14
Figure 7: Annual median water clarity against total annual Burdekin River discharge (in 10 <sup>3</sup> ML) from 2003 – 2012 for the Burdekin region. Annual values calculated based on a water year (1st Oct – 30th Sept). ....	15
Figure 8: Annual median water clarity against annual load of total phosphorus by the Burdekin River from 2005 – 2011 for the Burdekin region. ....	16
Figure 9: Partial smoother effects of a) wave height (m), b) wave frequency (m), c) tidal range (m) and d) bathymetry on daily water clarity (m) from GAMMs. Data are based on one mean value for each day and each cross-shelf band. Shaded ribbon indicates 95% confidence bands and vertical bars in the top right corner depict the relative scaling of each subplot. ....	17
Figure 10: Raw (a, b), detrended values (c, d) and seasonal cycles (e, f) for average daily water clarity (a, c, e) and Burdekin River daily discharge (b, d, f) from 2002 through 2012 for the Burdekin region. ....	19
Figure 11: Detrended values for average daily Burdekin River daily discharge and water clarity in the Burdekin Region from 2002 through 2012. ....	20
Figure 13: Ten year long-term trend cycle in a) daily Burdekin River discharge and b) daily mean water clarity from 2002 through 2012 for the Burdekin region. The horizontal dashed line indicates an arbitrary split (mean value) between high and low values. ....	21
Figure 13: Ten year seasonal cycle in a) daily Burdekin River discharge and b) daily mean standardised photic depth from 2002 through 2012 for the Burdekin region. The blue line represents a $\beta$ -spline smoother. The light blue and wheat shaded underlays represent regions above the mean levels for discharge and below mean levels for water clarity respectively. Dashed vertical bars extend the region of high discharge values onto the water clarity trace. ....	22
Figure 14: Ten year seasonal cycle in daily Burdekin River discharge (a and b) and daily standardized mean photic depth (c and d) for the Burdekin region for the dry years (2002 – 2006) and the wet years (2006 – 2012). The blue line represents a $\beta$ -spline smoother and the grey line represents the (scaled) first order derivative of the smoothing function. The horizontal red and blue dashed lines indicate an arbitrary split (mean value) between high and low values for the dry and wet years, respectively. The light blue and wheat shaded underlays represent regions above the mean levels for discharge and below the 10-m Secchi depth GBRMPA guideline values (green line), respectively. Dashed vertical bars extend the region of high discharge values onto the water clarity trace. Following seasonal decomposition of the GAMM residuals, seasonal trends were re-centered to the mean of water clarity predicted from the GAMM. ....	23

## List of Tables

Table 1. Monthly and annual mean photic depth (in meters) as a measure of water clarity for each cross-shelf transect and the whole Burdekin Region.....	12
Table 2: Mean annual values of photic depth and the environmental drivers, wave height, wave frequency, tidal range, and discharges of freshwater, total suspended solids (TSS), particulate nitrogen (TN) and particulate phosphorus (TP). Data are based on ‘water years (1 <sup>st</sup> October – 30 <sup>th</sup> September). .....	16
Table 3: GAMM output: Relationship of photic depth (daily means of each of the five cross-shelf bands) to wave height, wave frequency, tidal rang and bathymetry .....	18

## Acknowledgements

We thank the State of Queensland’s Department of Environment and Heritage Protection for providing the wave rider buoy data, and the river flow and river nutrient load data, and the sea level observations data. We thank the Bureau of Meteorology for providing the rainfall data. The study was funded by the Australian Marine Institute of Marine Science, and the Australian Government’s National Environmental Research Program (NERP) Tropical Ecosystems (TE) Hub. We thank the NASA Ocean Biology Processing Group for both the SeaWiFS and MODIS-Aqua satellite-to-in situ matchups for the in situ Secchi depth data .

## Summary

Light availability is a key resource for photosynthetic benthos including algae and corals. Here we use a 10-year time series (2002-2012) of daily 1 km<sup>2</sup> data from the Moderate Imaging Spectroradiometer onboard Aqua (MODIS-Aqua) to investigate the time scales and processes affecting water clarity in tropical coastal waters of the central Great Barrier Reef, Australia. An algorithm quantifying 'Photic depth' from MODIS-Aqua (defined as the penetration depth for 10% of surface irradiance) was chosen as a measure of water clarity. Generalized additive mixed models were used to relate spatial and temporal variation in daily and annual values of photic depth to daily and annual values in river runoff, wave height, wave period, tidal range, and bathymetry. Mean annual water clarity was strongly related to the annual freshwater discharge of the large Burdekin River ( $R^2 = 0.65$ ), the main source of new nutrients and sediments onto the shelf. Water clarity was ~20% reduced in the wetter years 2007 – 2012 with major Burdekin floods compared to the four dryer years of 2002 – 2006. Across the shelf, photic depth was most strongly related to Burdekin discharge for inshore, lagoon and mid-shelf bands (correlation coefficients:  $R^2 = 0.55 - 0.64$ ), weaker within the coastal strip that is chronically turbid ( $R^2 = 0.44$ ), and very weak for outer shelf waters ( $R^2 = 0.24$ ). The data also suggested a strong intra-annual relationship between river discharge and water clarity trends. Averaged over the 10 years, the Burdekin River tended to start discharging in late December, peaked in early February, and declined to low levels in April. Water clarity (standardised for environmental drivers) was highest in September to December, and declined from December onwards over a period of 3 months, until reaching a minimum in March to May. After May, water clarity started to increase again monotonously over a period of ~5 months until it returned to its maximum levels in September/October. Regional daily mean water clarity was therefore reduced from its dry season maximum for an average of about 7 months after the Burdekin started discharging, including for at least ~4 months after the river discharges had subsided. The adverse river effects therefore lasted on average 5 to 8 months per year, but data also showed intra- and inter-annual capacity for water clarity to recover. The data therefore suggest that reducing terrestrial runoff of nutrients and sediments should measurably improve water clarity in the GBR. Such improvement would lead to significant ecosystem benefits for the GBR.

## Introduction

Understanding the effects of terrestrial runoff on coastal water clarity in coral reefs exposed to river discharges of nutrients and sediments is of key concern. Light availability is a key resource for photosynthetic organisms including benthic algae, seagrass and corals. Light availability relative to surface irradiance can be quantified by the 'photoc depth' ( $Z_{\%}$ ; units of m), with, for example,  $Z_{10\%}$  reflecting the depth where 10% of the surface irradiance (PAR, photosynthetic available radiation; units of  $\mu\text{E cm}^{-2} \text{s}^{-1}$ ) remains (Weeks *et al.* 2012; Lee *et al.* 2007). Photoc depth is dependent on light attenuation, i.e. the transparency of the overlying water column (Falkowski and Raven 1997), and hence can be used as a measure of water clarity (Lee *et al.* 2007), being diminished both by the suspension of fine (clay- and silt sized) abiotic and biotic particulate matter, as well as some dissolved substances.

In shallow waters, water clarity is adversely affected by the bottom resuspension of sediments from wind waves and tidal currents (Larcombe *et al.* 1995; Wolanski *et al.* 2005; Piniak and Storlazzi 2008; Storlazzi and Jaffe 2008; Storlazzi *et al.* 2009, Fabricius *et al.* 2013). The relationship between changes in terrestrial runoff and water clarity is less well established, with the notable exceptions of studies during flood plumes, and on decadal changes in water clarity in relation to anthropogenic loadings in the North Sea and Adriatic (Baric *et al.* 1992; Justic *et al.* 1995; Borkman and Smayda 1998; McQuatters-Gollop *et al.* 2009). Such decadal time series are rare in tropical coastal waters, except for studies in estuaries and embayments where river runoff can alter water clarity at sub-diurnal to seasonal time scales (e.g., Schoellhamer 1996, 2002; Chen *et al.* 2007).

Coral reef and seagrass ecosystems are particularly sensitive to water clarity as the growth and survival of corals and seagrasses, which build these ecosystems, are light-dependent. The Great Barrier Reef (GBR) is the worlds largest (>2000 km long) coral reef system, containing over 3000 individual coral reefs. The GBR is highly vulnerable to terrestrial runoff, because it is primarily located on a shallow (<80 m) and 40–200 km wide continental shelf, and >30 major rivers discharge sediments and nutrients from increasingly developed catchments into the lagoon. Most rivers are dry during most of the year and only discharge during the summer wet season (November to April). During such discharge events, river plumes carry high loads of particulate matter, so water clarity within the flood plumes is visibly reduced, as documented by available satellite images of acute river plumes (Figure 1, Brodie *et al.* 2010; Bainbridge *et al.* 2012). River discharges supply annually a mean of 17 million tonnes of suspended sediment, 80,000 tonnes



of nitrogen, and 16,000 tonnes of phosphorus (Kroon et al. 2012). Consequently, GBR sediments from the coast to about 20 m bathymetry are dominated by terrigenous materials, while offshore sediments consist mostly of biogenic carbonates (Belperio and Searle 1988). The silt and clay sediments of these discharges are transported by long-shore currents for tens to hundreds of kilometers northwards from the river mouths. Nepheolid flows and tropical cyclones can also shift significant amounts of coastal sediments into deeper offshore shelf zones (Gagan et al. 1990; Wolanski et al. 2003). However, both the intra- and inter-annual time scale of burial or export of such newly imported fine sediments (long-term dispersal of the particulate material and its residency time beyond the times of the acute floods) on the continental shelf remain poorly understood, although a recent literature review estimated it to be decades to centuries (Brodie et al. 2012). Water clarity is typically low in the near-shore zone along much of coast line (De'ath and Fabricius 2010, Weeks et al. 2012). In shallow water (<20 m bathymetry), the fine sediments undergo repeated cycles of resuspension and deposition, until they are eventually deposited either on the deeper seafloor below the reach of storm waves or in north-facing coastal embayments (Wolanski 1994; Larcombe et al. 1995; Wolanski et al. 2005; Lambrechts et al. 2008).

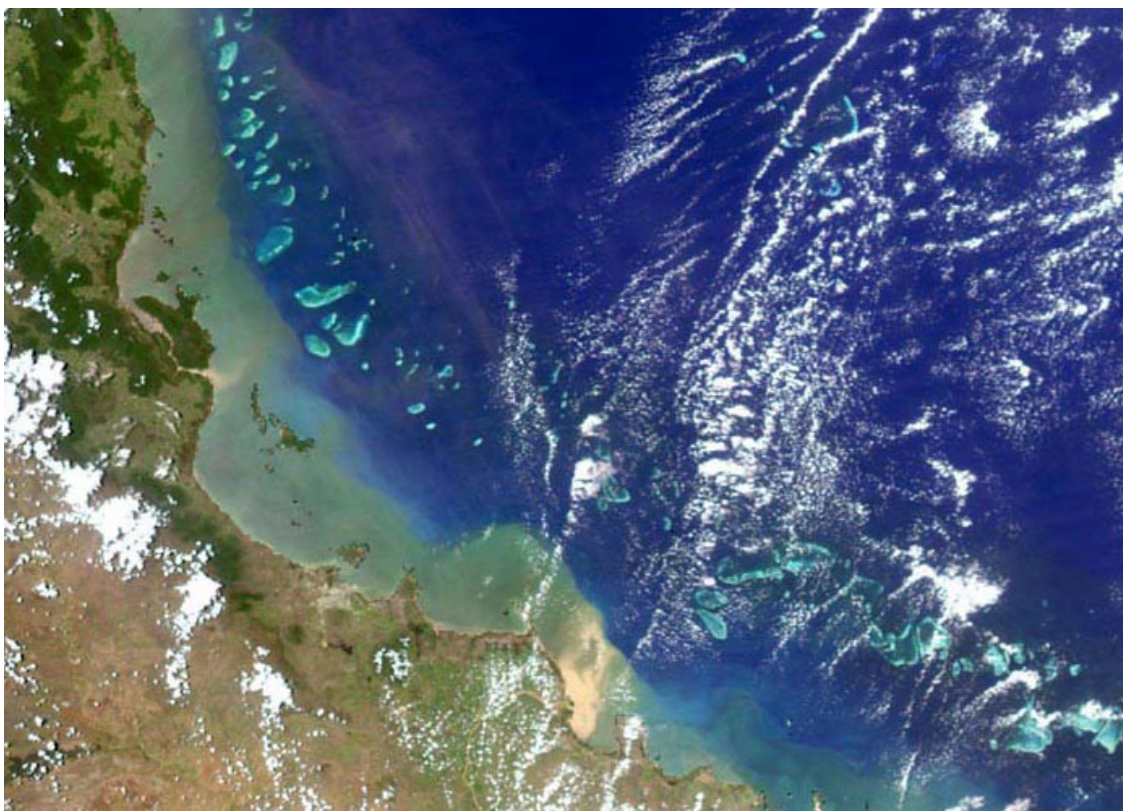


**Figure 1: MODIS-Aqua Image of the Burdekin Region during a moderate flood discharge event (10<sup>th</sup> February 2007). Image provided by NASA and processed by Matt Slivkoff.**

River loads of total suspended solids and nutrients have increased 3 – 8 fold compared to pre-European times (Kroon *et al.* 2012), and there is great concern that eutrophication and nutrient loads detrimentally affect GBR ecosystems (Brodie *et al.* 2009, De'ath and Fabricius 2010, Brodie *et al.* 2011). At chronically reduced water clarity, coral reefs experience shifts from phototrophic to heterotrophic systems, especially in deeper water, and a reduced lower depth limits of seagrass meadows (Loya 1976; Rogers 1979; Dennison 1985; Birkeland 1988; Babcock and Smith 2002; De'ath and Fabricius 2010). In coral reefs, loss of light from decreased water clarity, in combination with increased sedimentation rates, reduces coral growth rates, colony survival and settlement of new coral recruits (Rogers 1979; Babcock and Smith 2002). Low water clarity has also been associated with a five-fold increase in macroalgal cover and a 30% reduction in coral biodiversity (De'ath and Fabricius 2010), and increased bioerosion (LeGrand and Fabricius 2011). Moderately diverse coral communities with high coral cover can develop in highly turbid water, but are restricted to shallow waters (<2 m depth) and where sediment deposition rates are low (Cooper *et al.* 2007; Browne *et al.* 2010). Reduced water clarity also leads to a reduced depth distribution of corals and seagrasses, and a replacement of seagrasses with low-light tolerant macroalgae and phytoplankton (Dennison 1985; Duarte 1991; Cooper *et al.* 2007, Collier *et al.* 2012).

Substantial effort has therefore been made to reduce the terrestrial runoff of nutrients and sediments into the Great Barrier Reef, however effects have been predicted to become measurable in the marine environment only at a time scale of decades (Brodie *et al.* 2012, The State of Queensland and Commonwealth of Australia 2009) despite small recent reductions in end-of-river sediment and nutrient loads after farm management was improved under the Reef Rescue initiative (Queensland 2013). However, Fabricius *et al.* (2013) demonstrated that inshore water clarity remained reduced for weeks to months after the onset of the dry season after big river runoff events. They estimated that long-term mean turbidity was up to 10-fold higher on reefs near compared to away from river mouths. Additionally, inshore turbidity was on average 43% lower at the end compared to the start of the dry season on reefs with long-term mean turbidity >1.1 NTU, while turbidity returned to low levels within weeks after river flows and rainfall on reefs with long-term mean turbidity of <1.1 NTU. Their data suggested that the time scale of winnowing or consolidation of newly imported materials in the inshore zone is months to years, rather than years to decades. However, their 3-years record was too short to assess inter-annual variation in water clarity.

The present study used 10 years of remote sensing and environmental data (2002 – 2012) and statistical models, to assess whether daily to inter-annual variation in water clarity around coral reefs on a shallow continental shelf may be related to the terrestrial runoff of freshwater and its associated fine sediments and nutrients. The study also assessed the spatial extent (inshore to offshore) of and duration of periods of low water clarity beyond the duration of the flood plumes. The study shows that mean annual water clarity is strongly related to the freshwater discharge volumes of the Burdekin River, and is thus also related to its discharge of phosphorus and nitrogen. The study therefore suggests that low annual sediment and nutrient loads in the Burdekin River are likely to result in significantly improved water clarity downstream of the river mouth and across much of the continental shelf during the wet season and throughout the following dry season. We discuss the ecological benefits of this documented relationship between river loads and water clarity in the central Great Barrier Reef.

## Methods

### MODIS data: Photic depth

For this study, water clarity was determined by using a regionally-tuned photic depth algorithm applied to MODIS-Aqua data to determine the depth where 10% of the surface light (PAR) level is still available,  $Z_{10\%}$  (Weeks *et al.* 2012). The GBR-validated  $Z_{10\%}$  algorithm was derived from a quasi-analytical algorithm based on the inherent optical properties, a function of absorption and backscattering, of the water column (Lee *et al.* 2007). The algorithm was developed and validated through regression with over 5000 records of Secchi depth ( $Z_{SD}$ ) that were collected by the Australian Institute of Marine Science and the Queensland Department of Primary Industries and Fisheries between 1994-1999 and 1992-2012. Many of the  $Z_{SD}$  data (collected) pre-dated the MODIS-Aqua satellite data (2002-2012), hence Sea-viewing Wide Field-of-view Sensor (SeaWiFS) data (1997-2010) were also used to validate and improve the photic depth product for the GBR ecosystem. The satellite-to-in situ matchups for the in situ  $Z_{SD}$  dataset were acquired from the NASA Ocean Biology Processing Group for both SeaWiFS and MODIS-Aqua. Stations in optically shallow water, where the signal is affected by light reflection from the sea floor, were excluded.

A regression of the in situ  $Z_{SD}$  values against the matching satellite estimates of  $Z_{10\%}$  was used to adjust the satellite-derived  $Z_{10\%}$  to  $Z_{SD}$ , to determine GBR  $Z_{10\%}$ . A Type II linear regression of log-transformed satellite and in situ data was used to estimate  $Z_{10\%}$  ( $=Z_{SD}$ ) for the GBR according to:

$$\text{GBR } Z_{10\%} = 10^{\{[\log_{10}(Z_{10\%}) - a_0] / a_1\}}$$

where  $a_0$  and  $a_1$  are 0.518 and 0.811 [slope and intercept] for SeaWiFS and 0.529 and 0.816 for MODIS-Aqua. Finally, this GBR-validated photic depth algorithm was implemented into the NASA satellite processing software (SeaDAS) and applied to the full time series of MODIS-Aqua data (1<sup>st</sup> July 2002- 21 November 2012).

Using bathymetry data for the GBR shelf, a mask was generated for the Burdekin NRM region (~17.9-20.1°S and 146.3-149.3°E, 0 to -200 m), excluding reefs (Figure 3). The final data contained 25,621 grid points at 1-km<sup>2</sup> resolution. Data availability varied greatly between months due to cloud cover.

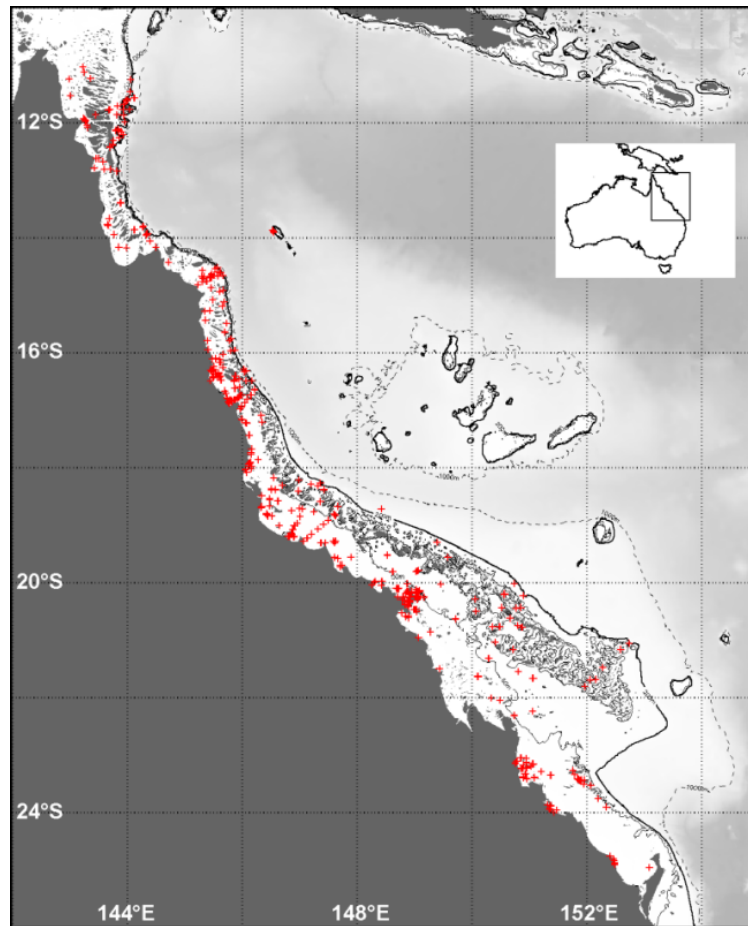


Figure 2: Map of the Great Barrier Reef, with the Secchi data stations used for calibration marked as red crosses.

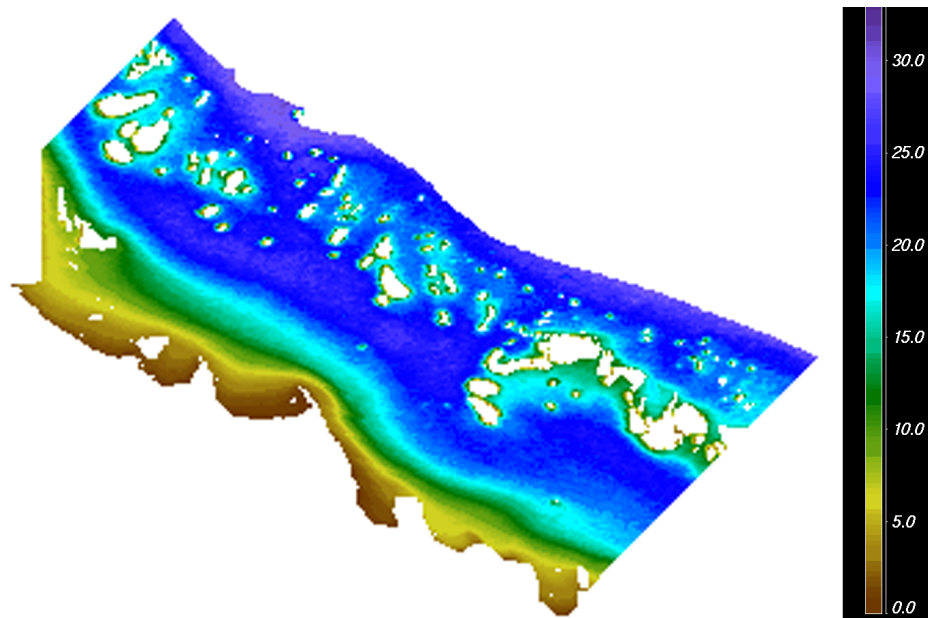


Figure 3: The spatial extent of the Burdekin Region, and an example of spatial patterns in photic depth within the Burdekin NRM Region. The colour contours indicate mean photic depth for September.

## Environmental data

Environmental data were obtained as follows: The bathymetry (as metres below astronomical tide) data for each RS pixel were obtained from a high-resolution digital elevation model (DEM) for the GBR and adjoining Coral Sea at a grid pixel resolution of 0.001-arc degree (about 100 m) (Beaman 2012). Daily data of freshwater discharge volumes of the Burdekin River were supplied by the Queensland Department of Environment and Heritage Protection (DEH; Figure 5). Data on loads of suspended solids were obtained from Kuhnert *et al* 2012). In the Burdekin River, the relationship between freshwater volume and sediment loads is moderate ( $R^2 = 0.58$  for 2002 – 2012; Kuhnert *et al* 2012). Hourly data on wave height and wave frequency data from a wave rider buoy located 8 km northeast of Cape Cleveland (Latitude: 19° 09.583'S Longitude: 147° 03.457'E) were provided by DEH. Data on daily tidal amplitudes as a proxy for tidal currents (one daily value for the whole region) were calculated from hourly predicted sea level data derived from a storm tide gauge site in Townsville Harbour (Latitude : 19° 15.23' S Longitude : 146° 49.77' E), provided by DEH. Gaps in the tidal range data, were imputed from estimates generated from a harmonic tide clock and tide predictor (Flater, 2005: Tide; <http://www.flaterco.com/xtide/>) after correcting for an offset calculated over all available tide measurements.

## Statistical analyses

As the wet season in the GBR extends from October to about April the following calendar year, annual means were calculated based on 'water years' (01<sup>st</sup> October – 30<sup>th</sup> September). Relative distance across and along the shelf was calculated for each of the 25,621 remote sensing pixels. Mean photic depth was calculated for the whole data set, and for each of five transects across the shelf (distance proportional to the width of the continental shelf: coastal: 0-0.1 across, inner: 0.1-0.25 across, lagoon: 0.25-0.45 across, midshelf: 0.45-0.65 across, outer shelf: >0.65 across, Figure 4).

The procedure was to fit a generalized additive mixed effects model relating ln-transformed photic depth to penalized  $\beta$ -spline smoothers, representing the effects of wave height (ln), wave frequency (ln), tidal range and bathymetry. Smooth components were treated as random effects. Wind speed was not included, since it had a substantial data gap, was highly correlated with waves and likely a more indirect predictor for water clarity than wave height. Similarly, rainfall is highly correlated with river flow and was therefore excluded.

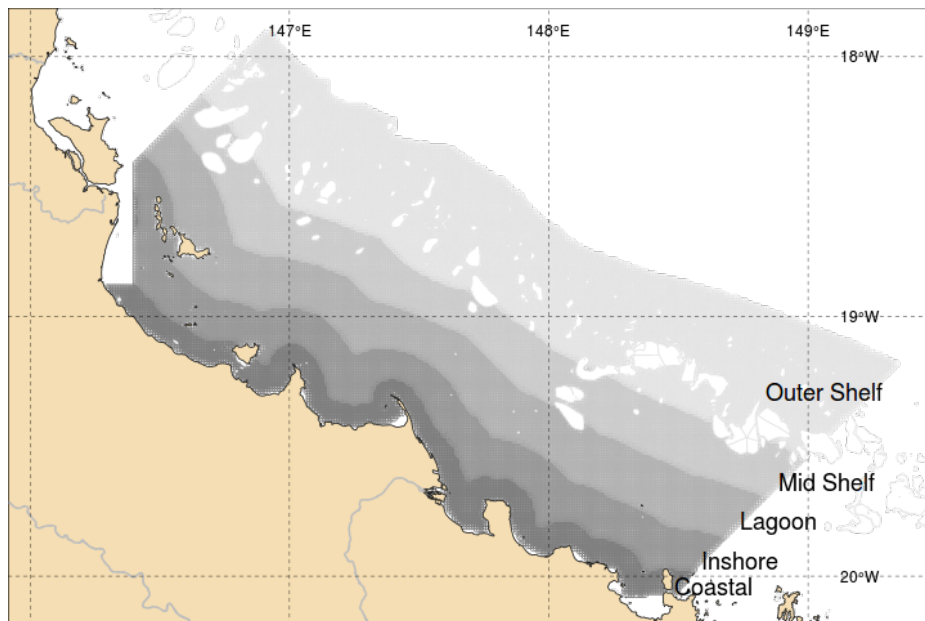


**Figure 4: The five transects across the shelf (coastal: 0-0.1 across, inner: 0.1-0.25 across, lagoon: 0.25-0.45 across, midshelf: 0.45-0.65 across, outer shelf: >0.65 across).**

Time series traces of photic depth as well as the various environmental data were initially explored to identify and diagnose issues with any of the series as well as confirm the existence of cyclical (seasonal) patterns.

Cross-correlation lags between daily photic depth and the main environmental drivers were calculated to determine the potential scale and pattern of temporal offsets. These cross-correlations revealed that there was a substantial and very blunt lag associated with Burdekin River discharge. This implies that any potential causal links between photic depth and river discharge are delayed and accumulative over prolonged periods rather than instantaneous pulses. Consequently, river discharge impacts are more appropriately modeled as seasonally detrended long-term trends against similarly detrended photic depths.

The overall association between photic depth and Burdekin River discharge was explored by correlating annual median photic depth (calculated across the entire region) against the annual total Burdekin River discharge, where annual summaries were based on water years. Similarly overall associations were also calculated between photic depth and total suspended solids (TSS), particulate nitrogen (TN) and particulate phosphorus (TP). However, TSS, TN and TP were all highly correlated to each other as well as to the total volume of water discharged, compromising the ability to investigate the main factors reducing water clarity.



Generalized Additive Mixed Models (GAMMs; (Wood 2006) were used to explore the nature of relationships between photic depth and a range of climatic and maritime predictors. Specifically, a GAMM model was used to relate ln-transformed photic depth to penalized  $\beta$ -spline smoothers, representing the effects of wave height (ln), wave frequency (ln), tidal range and bathymetry. GAMMs are an extension of additive models (which allow flexible modelling of non-linear relationships by incorporating penalized regression spline types of smoothing functions into the estimation process) in which the degree of smoothing of each smooth term (and by extension, the estimated degrees of freedom of each smoother) is treated as a random effect and thus estimable via its variance as with other effects in a mixed modelling structure (Wood 2006). In the present study the basis of the smoothing functions were represented by penalized  $\beta$ -splines (Eilers *et al.* 1996).

Spatial and temporal autocorrelation was explicitly modelled by including the sub-regions as random effects and incorporating a first-order autoregressive correlation structure (Pinheiro and Bates 2000). Normality was checked and ln-transformations were used to normalize photic depth, wave height and wave frequency. Modelling against a gaussian distribution greatly reduced the computational effort and convergence issues compared to a Gamma distribution.

The residuals from the GAMM (which thus reflect the photic depth signal after the extraction of wave, tidal and bathymetry signals) were seasonally decomposed to derive the seasonal and long term trends (2002-2013) in photic depth throughout the Burdekin region. Seasonal decomposition applies a smoother (typically either a moving average or locally weighted regression smoother) through a time series so as to break the series into its underlying seasonal factors (periodic fluctuations due to cyclical reoccurring influences) and trend cycle (long-term trends) (Kendall M and A 1983). Such decomposition is represented mathematically as:

$$Y_t = f(S_t, T_t, E_t),$$

where  $Y_t$ ,  $S_t$ ,  $T_t$  and  $E_t$  are the observed value, seasonal, trend cycle and irregular (residual) components, respectively, at time  $t$ .

Additive decomposition models are appropriate when the magnitude of seasonal fluctuation is relatively constant, whereas multiplicative models are better suited when the degree of seasonal fluctuation increases with increasing seasonal level. As the residuals from a Gaussian model are always zero centered and since the response variable was log-transformed, the residuals are on



a log scale. Thus following temporal decomposition, trend and seasonal cycles were re-centered around mean GAMM fitted values and transformed back into the original photic depth scale via exponentiation.

Similarly, patterns in daily Burdekin River discharge values were also seasonally detrended. Long-term water clarity trends were hence cross-correlated against long-term river discharge trends. Effect sizes (rate of change in long-term water clarity per unit change in long-term discharge) are expressed as a percentage of initial water clarity as well as  $R^2$  value were calculated.

To explore spatial differences in the temporal associations of long term photic depth and Burdekin River discharge trends, a series of GAMM's and seasonal decompositions were performed separately for each sub-region (coastal, inner, lagoon, midshelf and outer shelf). In each case, photic depth data comprised daily measurements from each of four points. Each point was selected from along one of four transects running perpendicular to the coast and spaced approximately equally from North-South.

The analyses were also performed separately for dry (2002-2006) and wet (2007-2012) years so as to further investigate the differences in seasonal fluctuations in adjusted photic depths associated with spans of either low or high levels of Burdekin River discharge respectively.

All GAMMs were fitted using the mgcv (Wood 2006, Wood 2011) package in R 2.15.1 (Team 2013).

## Results

### Spatial and seasonal patterns in photic depth

The raw daily recorded values of mean region-wide photic depth derived from the remote sensing data, as well as daily rainfall, Burdekin River discharge, wind speed, wave height, wave frequency and maximum daily tidal range are shown in Figure 5. Strong seasonal cyclic structures were apparent in photic depth, rainfall and river runoff and daily tidal ranges. Daily rainfall was highly correlated with the Burdekin River discharges, and so were the discharges of the Houghton, Ross and Black Rivers. Wind speed was highly correlated with wave height and wave frequency. For these reasons, rainfall, the discharges of the small rivers, and wind speed were not further analysed.

Spatial and seasonal differences in photic depth were strong, with almost four times greater annual mean photic depth encountered in the offshore compared with the coastal transect (annual mean: 15 m vs. 4 m; Table 1). Seasonally, photic depth was greatest in August to December and lowest in March to May (regional mean: 12.6 – 13.9 m, and 8.61 – 8.8 m, respectively; Table 1).

**Table 1. Monthly and annual mean photic depth (in meters) as a measure of water clarity for each cross-shelf transect and the whole Burdekin Region.**

<b>Shelf</b>	<b>Jan</b>	<b>Feb</b>	<b>Mar</b>	<b>Apr</b>	<b>May</b>	<b>Jun</b>	<b>Jul</b>	<b>Aug</b>	<b>Sep</b>	<b>Oct</b>	<b>Nov</b>	<b>Dec</b>	<b>Annual Mean</b>
Coastal	4.41	3.57	3.25	3.07	3.38	3.73	3.94	4.25	4.11	3.99	4.61	4.92	<b>3.94</b>
Inshore	8.97	7.72	6.31	6.32	6.68	7.30	8.68	10.5	10.87	9.52	9.71	10.4	<b>8.58</b>
Lagoon	13.40	12.17	9.66	9.56	9.94	10.81	13.0	16.1	17.9	16.5	15.7	17.1	<b>13.5</b>
Midshelf	13.90	12.25	10.71	10.54	10.86	11.77	13.3	16.1	18.3	16.7	16.0	16.4	<b>13.9</b>
Outer shelf	15.39	14.18	13.52	13.55	13.39	13.57	14.0	16.2	18.5	17.5	17.6	17.1	<b>15.4</b>
<b>Regional mean</b>	<b>11.21</b>	<b>9.98</b>	<b>8.69</b>	<b>8.61</b>	<b>8.85</b>	<b>9.44</b>	<b>10.6</b>	<b>12.6</b>	<b>13.9</b>	<b>12.9</b>	<b>12.7</b>	<b>13.2</b>	<b>11.1</b>

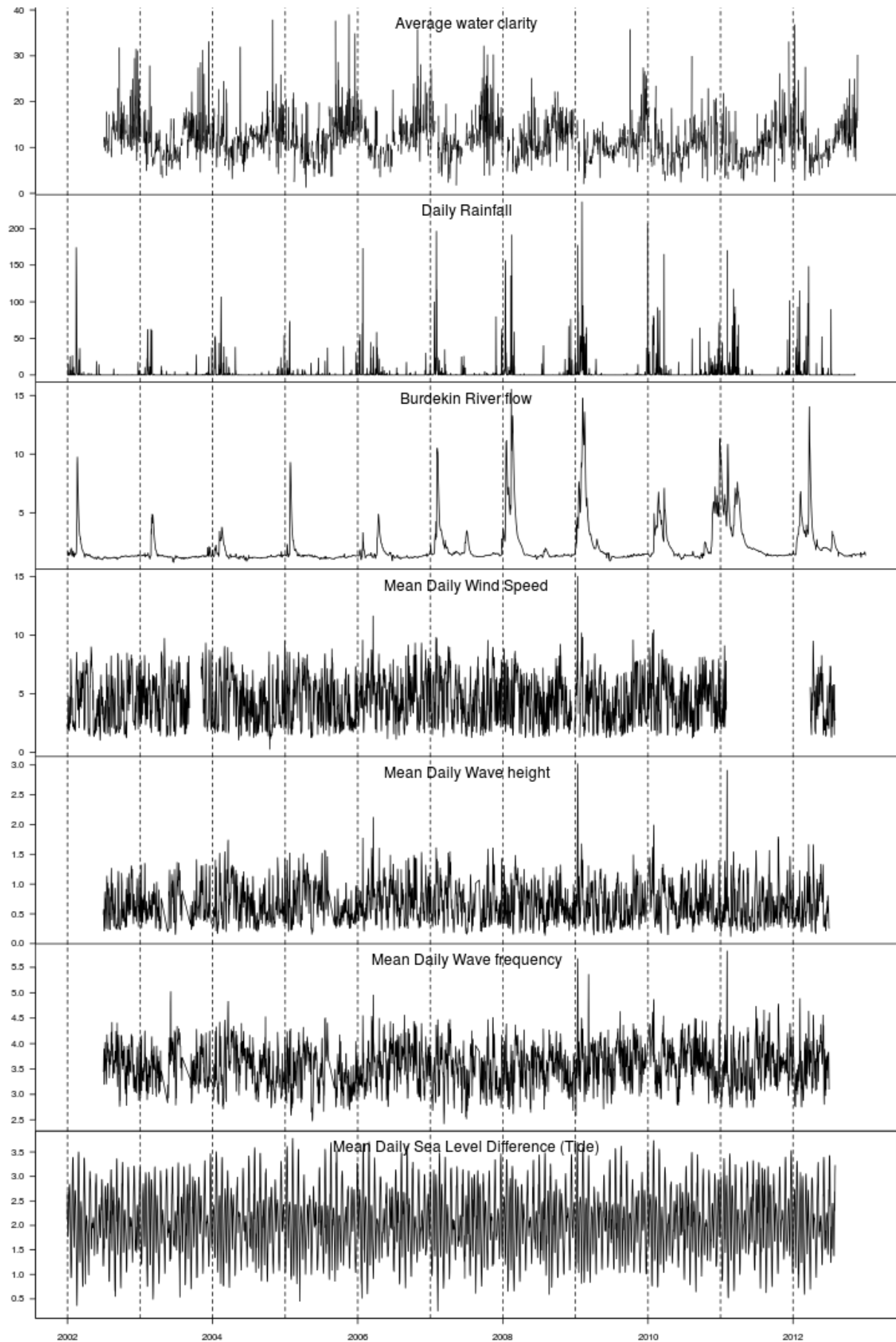
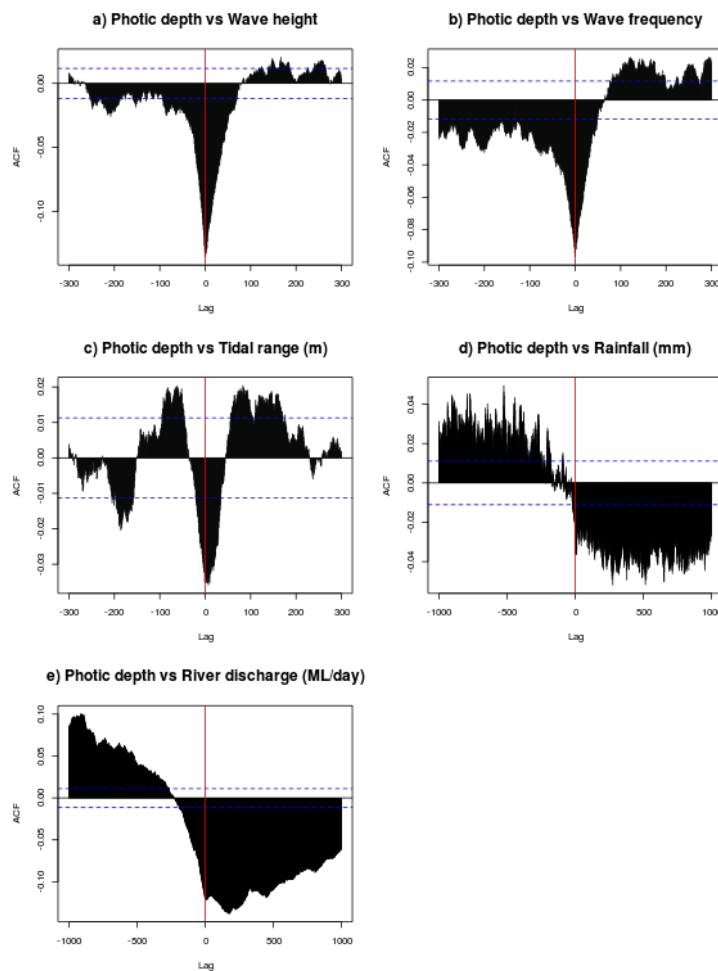


Figure 5: Time series traces of daily trends in region-wide water clarity, and climatic and river variables.

## Relationship of photic depth to environmental drivers: Lag effects

Cross-correlation lags for daily photic depth in relation to the main environmental drivers suggested that wave height and frequency and tidal range all had a maximum lag of 0 days (Figure 6). In contrast, cross-correlations between photic depth and Burdekin River discharge had more complex lag patterns, possibly suggestive of a maximum lag of approximately 0-100 days (0-3+ months). This suggests that wave and tidal drivers affect water clarity more or less instantaneously (brief pulse impacts), and the effects are not maintained by more than a few days. In contrast, i.e., river discharge effects on water clarity appeared to manifest themselves as more accumulated and sustained impacts ((lasting chronic impacts), with delayed onset and being maintained over an extended temporal scale.



**Figure 6: Cross-correlation lags for daily water clarity against various environmental drivers a) Wave height (m), b) Wave frequency, c) Tidal range (m), d) Rainfall (mm) and e) Burdekin River discharge**

### Relationship of photic depth to environmental drivers: Changes in annual mean photic depth (averaged across the whole Burdekin region)

Time series of raw annual regional means in water clarity, unadjusted for any of the environmental drivers, are shown in Figure 7. There were strong differences in the discharge volume of freshwater by the Burdekin River between the years, with five dry years (2002 – 2006) being followed by six relatively wetter years (2007 – 2012). The year 2002 was excluded from the correlation analysis as the MODIS-Aqua data series started 1<sup>st</sup> July and hence represented an incomplete water year (starting 1<sup>st</sup> October).

Annual mean water clarity was strongly related to annual Burdekin discharges of freshwater ( $R^2 = 0.65$ ; Figure 7). The relationship was weaker for the loads of total phosphorus ( $R^2 = 0.51$ ), and weak for total nitrogen ( $R^2 = 0.33$ ) and total suspended solids ( $R^2 = 0.14$ ). However, the latter statistics are unreliable as they were based on incomplete data sets (Table 2): for TP and TN, no load data were available for the years 2002 – 2004 and 2012, and for TSS, the load estimates for different years were derived from different sources (2003 – 2009: Kuhnert et al. 2012, else: DERM), likely affecting comparability. Although the analysis suggests that water clarity was reduced by 1.7% for each 1000 t of TP discharged into the GBR, and by 0.47% for each 1000 t of TN discharged into the GBR, this assessment is again unreliable due to the highly correlated nature of concentrations of these materials.

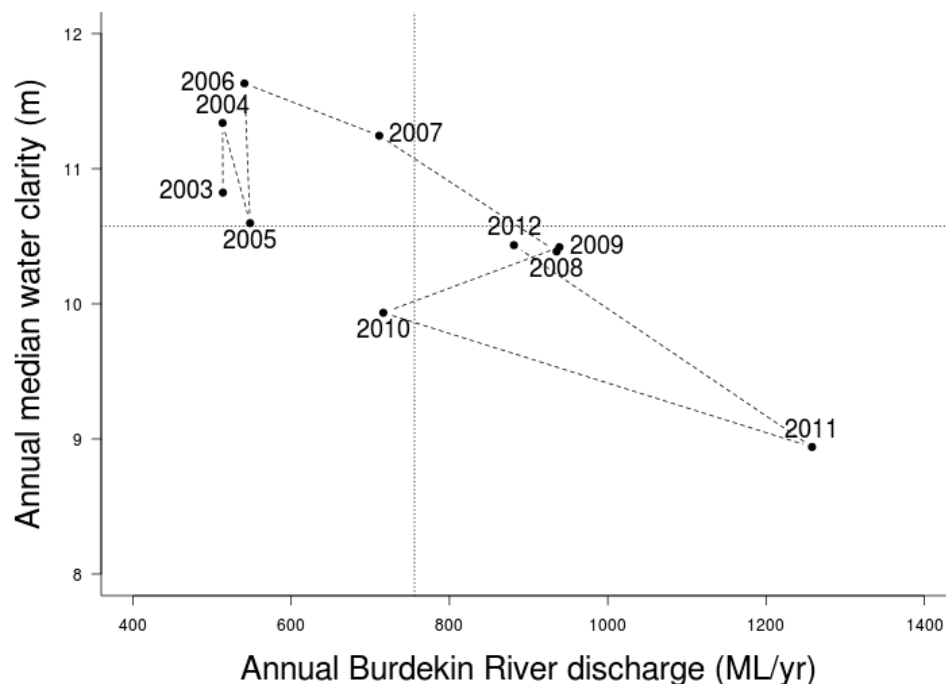


Figure 7: Annual median water clarity against total annual Burdekin River discharge (in  $10^3$  ML) from 2003 – 2012 for the Burdekin region. Annual values calculated based on a water year (1st Oct – 30th Sept).

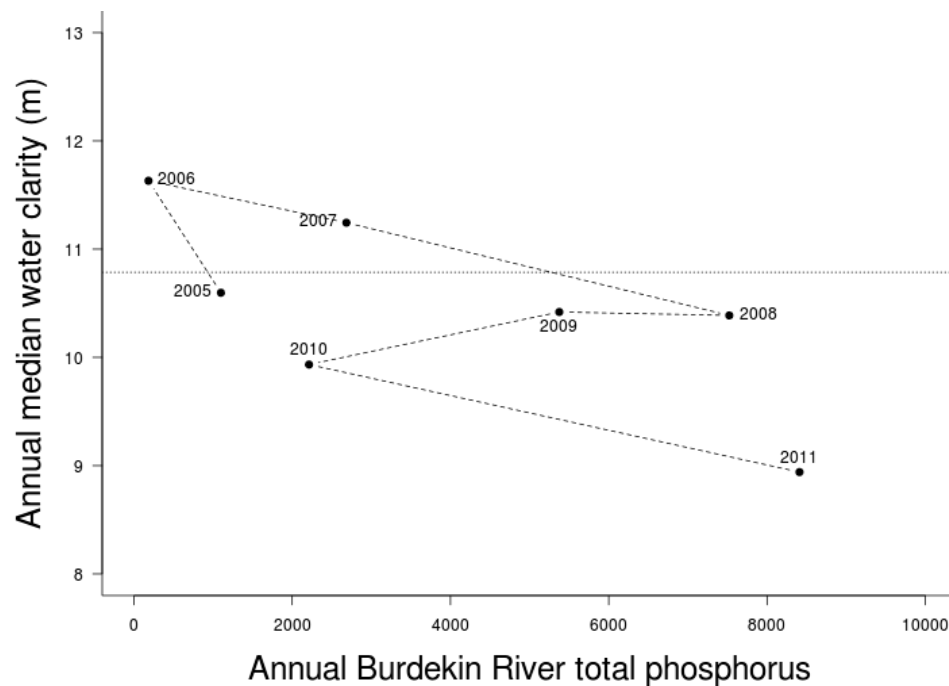


Figure 8: Annual median water clarity against annual load of total phosphorus by the Burdekin River from 2005 – 2011 for the Burdekin region.

Table 2: Mean annual values of photic depth and the environmental drivers, wave height, wave frequency, tidal range, and discharges of freshwater, total suspended solids (TSS), particulate nitrogen (TN) and particulate phosphorus (TP). Data are based on 'water years (1<sup>st</sup> October – 30<sup>th</sup> September).

Water Year	Photic Depth (m)	Wave Height (m)	Wave Frequ (s)	Tidal Range	Freshwater (10 <sup>3</sup> ML)	Burdekin River		
						TSS (1000 t)	TN (t)	TP (t)
2002	NA	0.502	3.71	2.11	106.21	2,141	NA	NA
2003	10.8	0.601	3.57	2.09	513.79	755	NA	NA
2004	11.3	0.645	3.60	2.10	513.37	384	NA	NA
2005	10.6	0.679	3.44	2.12	548.13	4,338	4,500	1,100
2006	11.6	0.629	3.50	2.07	540.97	884	1,600	185
2007	11.3	0.623	3.54	2.08	711.27	7,195	7,826	2,685
2008	10.4	0.648	3.53	2.12	935.35	14,806	26,528	7,523
2009	10.4	0.577	3.55	2.14	938.91	10,855	18,504	5,375
2010	9.93	0.642	3.70	2.08	716.45	2,485	6,411	2,213
2011	8.94	0.585	3.53	2.14	1258.07	6,167	2,1450	8,410
2012	10.4	0.606	3.61	2.11	881.43	NA	NA	NA
2013	13.0	NA	NA	NA	71.98	NA	NA	NA

Water clarity is most likely correlated to fine sediment ( $< 10\mu\text{m}$ ) inputs rather than the coarser fractions. As the models were run against total SS the correlations were likely to be weaker due to this factor. Fine sediments interact with nutrients in the Burdekin discharge plume forming organic rich flocs (Bainbridge et al. 2012) which are easily resuspendable after deposition. The Burdekin River now has a greater proportion of fine sediment in its discharge due to the construction of the Burdekin Falls Dam which traps most of the supply of coarser sediment fractions (Lewis et al. 2013).

### Relationship of photic depth to environmental drivers: Changes in daily mean photic depth (averaged across the whole Burdekin region)

A GAMM fitted to the daily data showed strong instantaneous effects of wave height, wave frequency, tidal range and bathymetry on individual daily water clarity values on a mean of the five cross-shelf transects (Table 3, Figure 9). Burdekin discharge was not included in this analysis of instantaneous effects, due to the observed longer lag phase between discharge and water clarity. Not surprisingly, mean daily wave height and bathymetry were very strong predictors of daily water clarity. In contrast, daily wave frequency (which is strongly related to wave height) was the weakest predictor, and daily tidal range contributed in a minor way. The model explained 74% of the variation in the data.

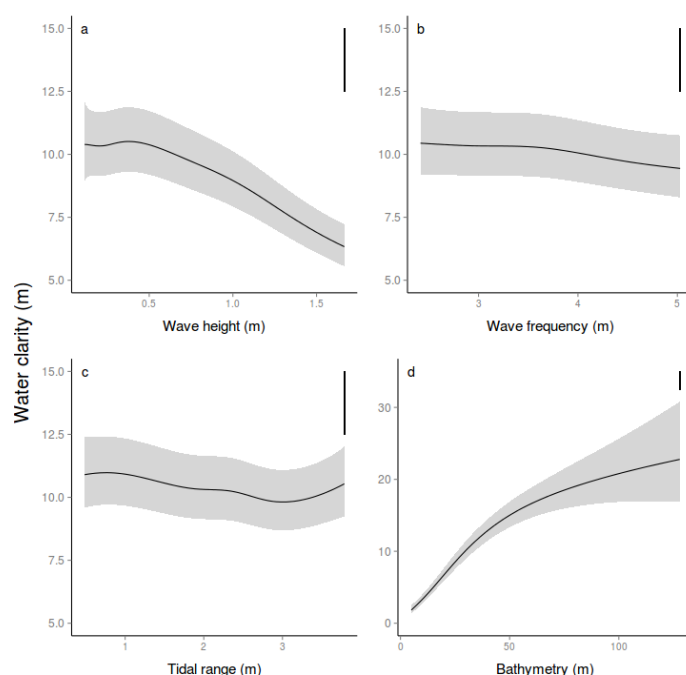


**Figure 9: Partial smoother effects of a) wave height (m), b) wave frequency (m), c) tidal range (m) and d) bathymetry on daily water clarity (m) from GAMMs. Data are based on one mean value for each day and**

each cross-shelf band. Shaded ribbon indicates 95% confidence bands and vertical bars in the top right corner depict the relative scaling of each subplot.

**Table 3: GAMM output: Relationship of photic depth (daily means of each of the five cross-shelf bands) to wave height, wave frequency, tidal range and bathymetry**

Photic depth:

	df	Ref.df	F	p-value	
Wave Height	4.24	4.24	51.62	<0.0001	***
Wave Frequ.	1.51	1.51	7.23	0.0022	**
Tidal Range	1.00	1.00	40.98	<0.0001	***
Bathymetry	3.90	3.90	2231.47	<0.0001	***

### Seasonal decomposition: Inter-annual patterns

The following analyses were conducted on the residual daily water clarity values for each of the cross-shelf transects, after having removed the effects of wave height, wave frequency, tidal range and bathymetry. Also, region-wide seasonal decomposition was used to remove the seasonal and moon cycle components of the time series. Once seasonal cycles (Figure 10a) were removed, the analysis showed particularly pronounced discrete minima in residual values many of which seemed to be aligned with the spikes in the raw and unadjusted maxima of the Burdekin freshwater discharge volumes (Figure 10b). Across years, mean water clarity was strongly related to Burdekin discharges ( $R^2 = 0.65$ ). There was a distinct gradual decline from large (8.5 m) to smaller (6.5 m) mean photic depth, with some periods of minor recovery in between, and a minimum in the year 2011. At the same time, Burdekin discharge rates increased from low to higher values, with a maximum in 2011 (Figure 10c and d). Standardisation (i.e. removal of wave and tidal effects) smoothed the curve slightly but did not affect the overall patterns, suggesting relatively minor difference in waves and tidal ranges between years (Figure 10c). The main relationship of interest from this analysis is once more depicted in Figure 11.



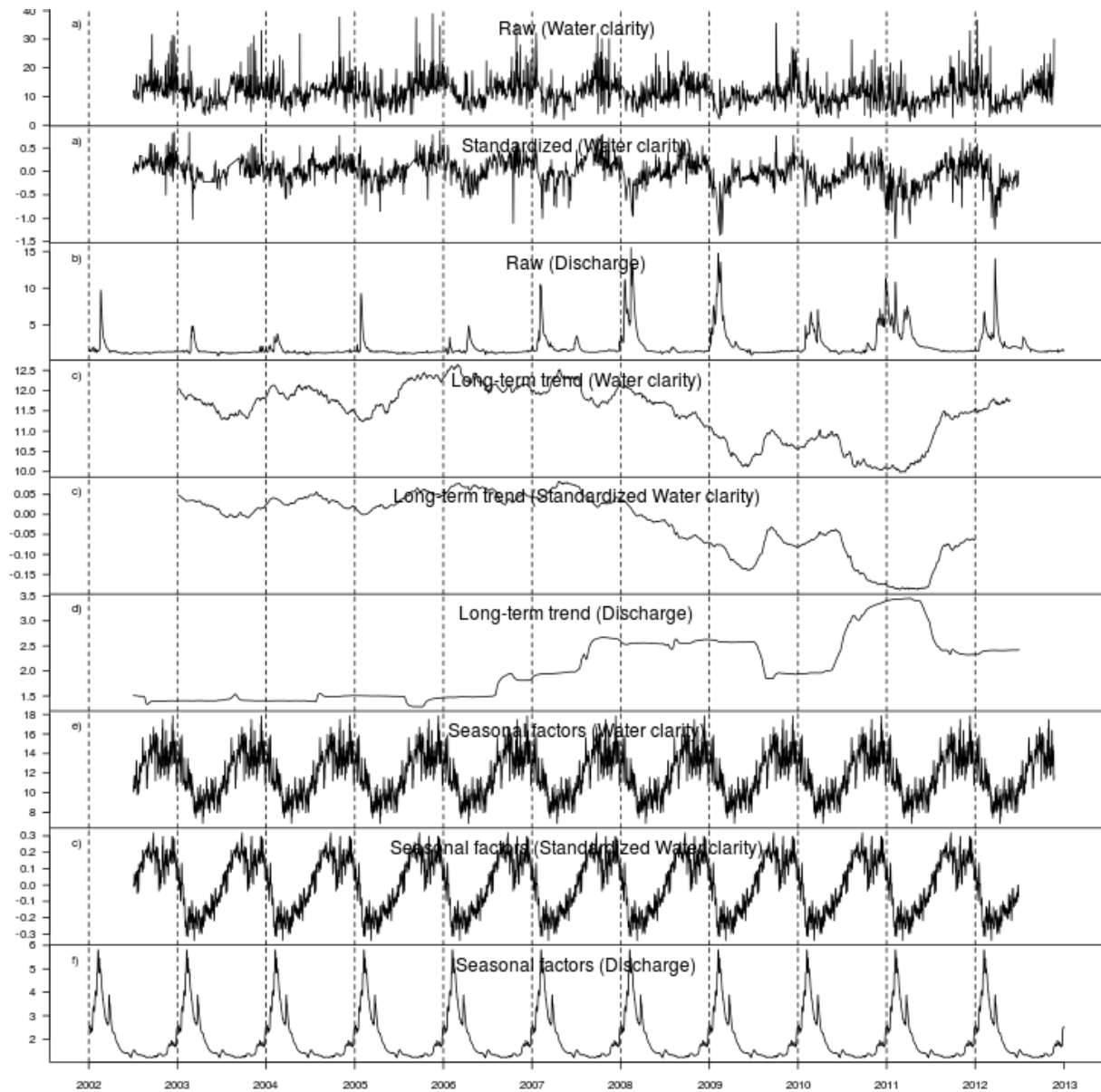
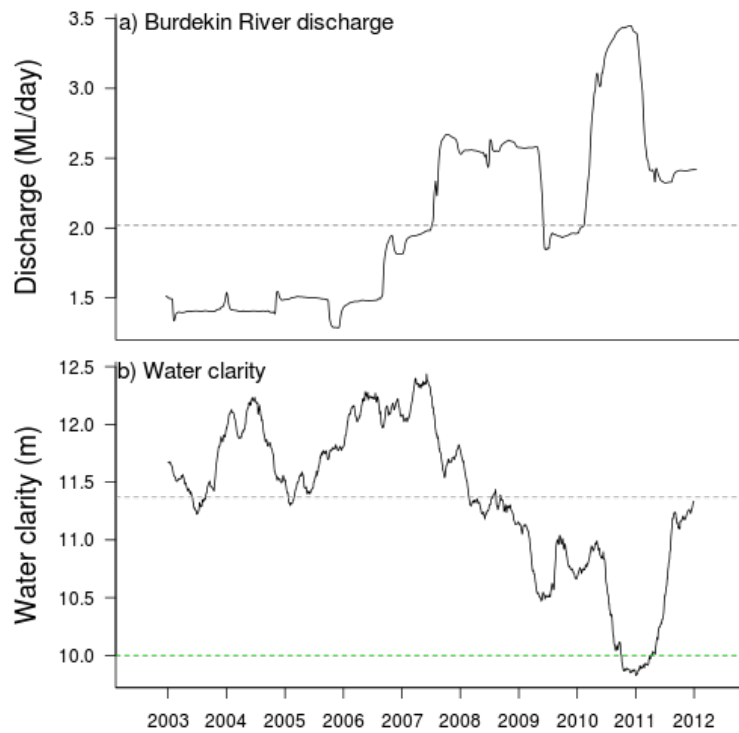
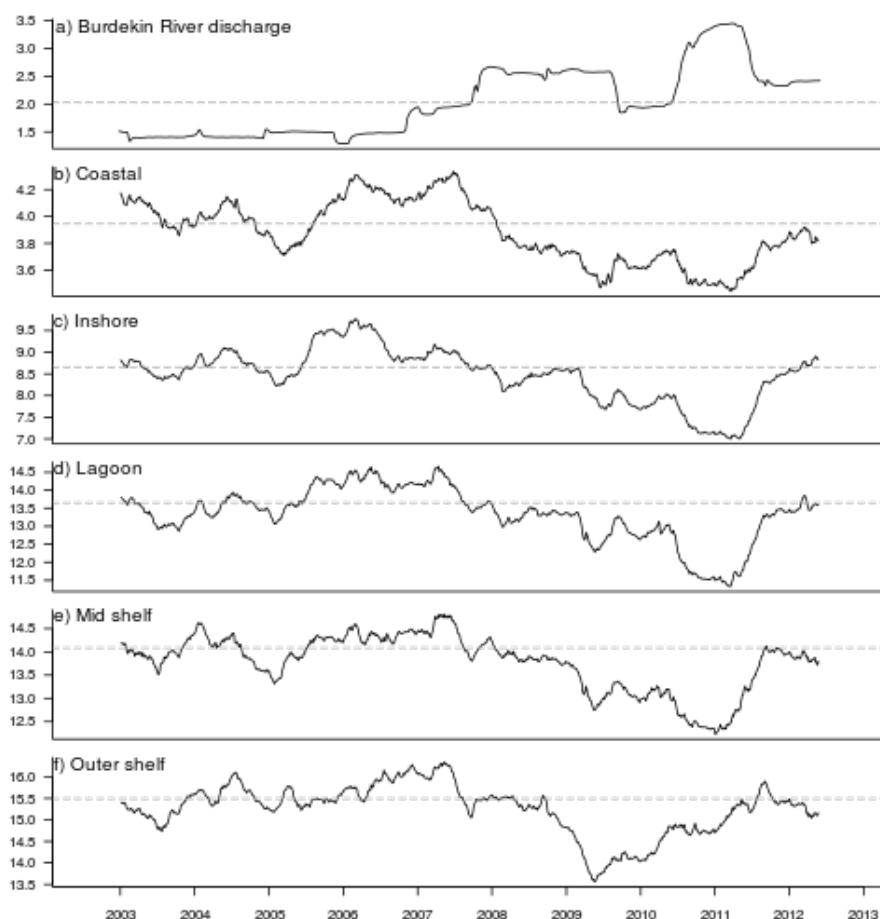


Figure 10: Raw (a, b), detrended values (c, d) and seasonal cycles (e, f) for average daily water clarity (a, c, e) and Burdekin River daily discharge (b, d, f) from 2002 through 2012 for the Burdekin region.



**Figure 11: Detrended values for average daily Burdekin River daily discharge and water clarity in the Burdekin Region from 2002 through 2012.**

To determine how the suggested river influence extended offshore, the above analyses were repeated for the five cross-shelf transects separately (Figure 4). The relationship of photic depth to Burdekin discharge values was strong for inshore, lagoon and mid-shelf bands (correlation coefficients: Inshore:  $R^2 = 0.61$ , Lagoon:  $R^2 = 0.64$ , Mid-shelf:  $R^2 = 0.56$ ), weaker within the coastal strip that is chronically turbid ( $R^2 = 0.45$ ), and very weak for outer shelf waters ( $R^2 = 0.24$ ) (Figure 12).



**Figure 12: Ten year long-term trend cycle in a) daily Burdekin River discharge and b) daily mean water clarity from 2002 through 2012 for the Burdekin region. The horizontal dashed line indicates an arbitrary split (mean value) between high and low values.**

### Seasonal decomposition: Intra-annual patterns

The mean intra-annual cycles (averaged over the ten years) also suggested a strong intra-annual relationship between river discharge and water clarity trends (Figure 13). The Burdekin River tended to start discharging in late December, peaked in early February, and declined to low levels in April. Water clarity, with environmental drivers removed, was highest in September to December, and declined from December onwards over a period of 3 months, until reaching a minimum in February to April/May. From there on, water clarity started to increase again monotonously over a period of ~5 months, and returned to its maximum levels in the late dry season (Table 1). Regional daily mean water clarity was therefore reduced from its dry season maximum for an average of about 7 months after the Burdekin started flowing, including at least ~4 months after the river discharges had subsided.

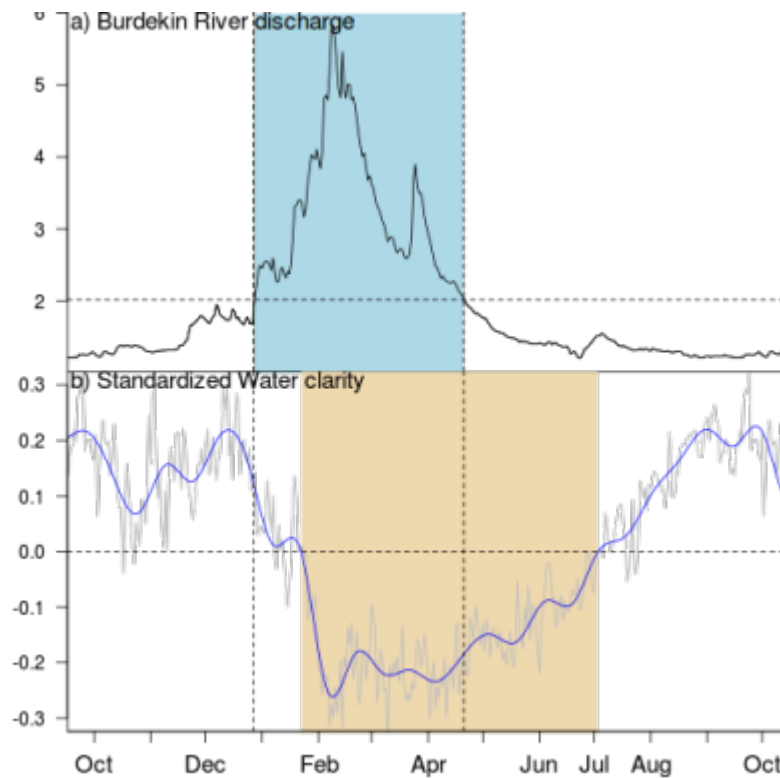


Figure 13: Ten year seasonal cycle in a) daily Burdekin River discharge and b) daily mean standardised photic depth from 2002 through 2012 for the Burdekin region. The blue line represents a  $\beta$ -spline smoother. The light blue and wheat shaded underlays represent regions above the mean levels for discharge and below mean levels for water clarity respectively. Dashed vertical bars extend the region of high discharge values onto the water clarity trace.

Figure 14). In the dry years, regional mean water clarity dropped below 10 m photic depth for 9 days, whereas in the wet years it was below 10 m for an average of 156 days per year. Mean daily water clarity was 19.79% lower in the wet compared to the dry years, although the values and timing of the individual peak and trough values, and the number of days of decline and recovery were similar.

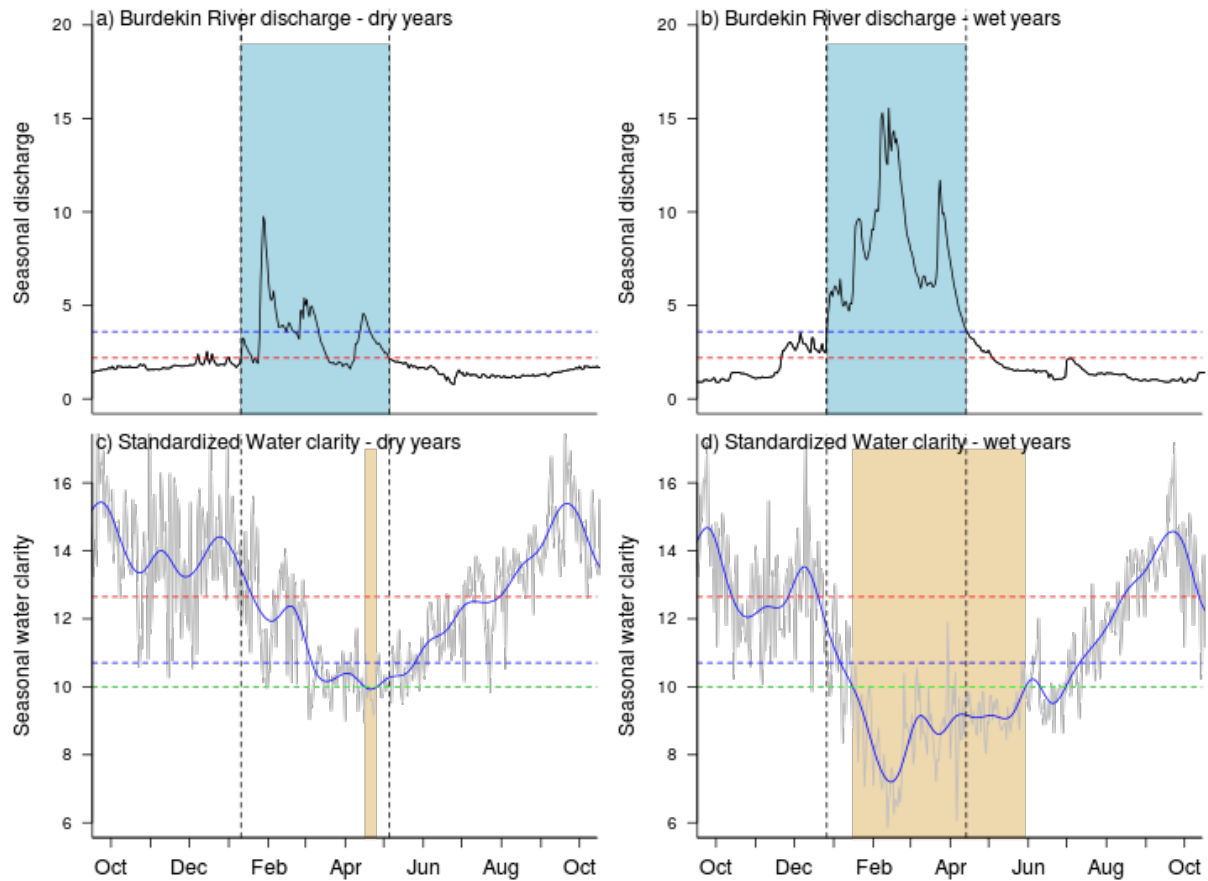


Figure 14: Ten year seasonal cycle in daily Burdekin River discharge (a and b) and daily standardized mean photic depth (c and d) for the Burdekin region for the dry years (2002 – 2006) and the wet years (2006 – 2012). The blue line represents a  $\beta$ -spline smoother and the grey line represents the (scaled) first order derivative of the smoothing function. The horizontal red and blue dashed lines indicate an arbitrary split (mean value) between high and low values for the dry and wet years, respectively. The light blue and wheat shaded underlays represent regions above the mean levels for discharge and below the 10-m Secchi depth GBRMPA guideline values (green line), respectively. Dashed vertical bars extend the region of high discharge values onto the water clarity trace. Following seasonal decomposition of the GAMM residuals, seasonal trends were re-centered to the mean of water clarity predicted from the GAMM.

This study demonstrated the strong dependency of water clarity across a shallow and wide tropical continental shelf of the central Great Barrier Reef on the river discharges both within and across years. The study confirmed waves and bathymetry to be strong determinants (Larcombe and Woolfe 1999, Anthony *et al.* 2004, Fabricius *et al.* 2013). Tidal effects were moderate, possibly reflecting the only moderate differences between smallest and largest tidal ranges within the Burdekin Region (~3 meters, Fabricius *et al.* 2013). By first testing for these environmental drivers using GAMMs, we were able to quantify and control for the daily effects of the environmental drivers and hence detect the strong underlying seasonal cycle in photic depth within this 10-years' time series. Once we accounted for the environmental drivers and the seasonal cycles, the strong relationship between mean annual water clarity and discharge volumes of the large Burdekin River became apparent. Across the whole shelf and averaged for whole water years, photic depth was almost 20% greater in four dry compared to six wet years.

Fabricius *et al.* 2013) showed that water clarity was linearly related to runoff, and that on turbid reefs it was on average 43% higher towards the end of the dry season compared with the beginning of the dry season. In other words, as the dry season progressed it required an increasing amount of wave and tidal energy to resuspend bottom sediments in the more turbid areas of the GBR. Three mechanisms may underpin this decline: (1) gradual movement of clays, silts and organic flocs by wind waves and tidal currents away from the shallow continental shelf where they are easily resuspendible, towards deeper waters or north-facing bays where resuspension requires higher wave and tidal velocities; (2) sediment compaction; and (3) declining plankton biomass after depletion of new nutrients and trace elements and into the cooler winter months (Brodie *et al.* 2007; Lambrechts *et al.* 2010).

(Fabricius *et al.* 2013) suggested the existence of an important threshold value: on reefs in relatively clear water (long-term mean of <1.1 NTU), water clarity was reduced during weeks with river flows and/or heavy rainfall, but returned back to baseline levels within weeks, suggesting removal or compaction of the unconsolidated newly imported silts and nutrients. In contrast, on reefs in more turbid waters (long-term mean of >1.1 NTU) water clarity took over 250 days in the dry season to gradually increase back to baseline values. On two of the most turbid reefs, this relationship was weak, due to high intra-annual variability, suggesting that on these reefs winnowing of new sediments may take more than one year, or that water clarity is not limited by modern sediment supply (Belperio 1983; Larcombe and Woolfe 1999). Indeed, thick deposits of predominantly terrigenous sediments along the coast and in particular

downstream of rivers confirm a net accumulation of sediments at geological time scales (Belperio 1983). The high long-term mean water clarity near rivers suggests that residual fine sediments remain available for resuspension for years after floods (Webster and Ford 2010; Lambrechts et al. 2010). More long-term water clarity data are needed to better quantify inter-annual changes in coastal and inshore water clarity in a region where river discharge volumes vary by more than one order of magnitude between years (Furnas 2003).

The apparent relationship of offshore water clarity to river discharges remains unresolved. Although plumes of the Burdekin River frequently cross the continental shelf (Bainbridge et al. 2012; Devlin et al. 2012, Schroeder et al. 2012) the material transported in the plumes to the mid and outer shelf is not well identified or quantified. However, high offshore water clarity during early spring has been attributed to a strengthening of the East Australian Current (EAC) and a relaxation of the southeast trade winds. This springtime acceleration of the EAC can lead to intrusions of clear nutrient-depleted oligotrophic offshore surface waters in the central GBR (Berkelmans et al. 2010), as well as to the intrusion of nutrient-enriched upwelled deeper waters. While these intrusions may contribute to explaining intra-annual differences in water clarity, they are unlikely to contribute significantly to explaining the differences between the wetter and dryer years in water clarity. Other processes that may also contribute to reducing water clarity may include the offshore transport of nepheloid materials - a process that is still poorly quantified, and seasonal changes in plankton. Chlorophyll is known to show strong seasonal variation, with mean concentrations being highest at the end of the wet season (March) and lowest in August, while also increasing with latitude and towards the coast (Brodie et al. 2007). The turbid coastal waters of the GBR (classified as 'Case 2') are typically dominated by abiotic suspended sediment particles and detritus rather than phytoplankton (Kirk 1991). Plankton blooms develop in response to the new nutrients and trace elements (e.g., iron) injected by terrestrial runoff (McKinnon and Thorrold 1993; Smith et al. 2003; Smith and Schindler 2009) or nutrient upwelling, and later on from the resuspension of bottom sediments that releases dissolved nutrients into the water column throughout the year (Walker 1981). An investigation of the contribution of phytoplankton and flocculation to water clarity will be essential to estimate the annual removal of sediments and nutrients from the pool of resuspendible seafloor material, and could become the basis of refined region-specific river load and coastal water quality targets.

In conclusion, this study clearly demonstrates that river discharges of sediments and nutrients significantly affect water clarity in the central Great Barrier Reef. The results of this study suggest

that a reduction in fine sediments and nutrient loads in the Burdekin Rivers is likely to lead to improved water clarity for at least 5 to 8 months of the year during and after the wet season, potentially also providing benefits into the following years. The effects of runoff on GBR water clarity documented here are sufficiently large to affect benthic coral reef communities. The summer wet season is the growing season for seagrasses, and seagrasses are light limited (Dennison 1985, Collier et al. 2012). The cover and biomass of seaweed such as *Sargassum*, which compete with corals for space, is in contrast strongly negatively related to water clarity (De'ath and Fabricius 2010), and again their main growing season is in summer. Also, the settlement of coral larvae tends to happen in early summer, with the young corals being most sensitive to sedimentation and poor water quality within the first few months after settlement. These and other examples demonstrate that any reduction in river loads that would lead to improved water clarity is likely to lead to significant ecosystem health benefits. Queensland's catchments show strong positive relationships between (a) vegetation cover and soil erosion in grazing lands, and (b) the proportion of land where fertilizer is applied and nutrient concentrations in river waters (Brodie et al. 2008; Hughes et al. 2009). Reducing losses of eroded soils and fertilizer to the rivers by vegetation management is therefore a key to managing coastal water clarity in the GBR, and improvements may be expected within intra- to inter-annual time scales.



## References

- Anthony K, Ridd PV, Orpin AR, Lough J (2004) Temporal variation of light availability in coastal benthic habitats: Effects of clouds, turbidity, and tides. *Limnol Oceanogr* 49:2201–2211
- Babcock RC, Smith L (2002) Effects of sedimentation on coral settlement and survivorship. *Proceedings of the Ninth International Coral Reef Symposium* 1:245–248
- Bainbridge Z, Wolanski E, Lewis S, Brodie J (2012) Fine sediment and nutrient dynamics related to particle size and floc formation in a Burdekin River flood plume, Australia. *Mar Pollut Bull* 65:236–248
- Baric A, Marasovic I, Gacic M (1992) Eutrophication phenomenon with special reference to the Kascaronetela Bay. *Chem Ecol* 6:51–68
- Beaman RJ (2012) Great Barrier Reef and Coral Sea bathymetry. ed. S. o. E. a. E. S. James Cook University. <http://deepreef.org>: <http://deepreef.org>.
- Belperio AP (1983) Terrigenous sedimentation in the central Great Barrier Reef Lagoon: a model from the Burdekin region. *BMR Journal of Australian Geology and Geophysics* 8:179–190
- Belperio AP, Searle DE (1988) Terrigenous and carbonate sedimentation in the Great Barrier Reef province. In: J. DL, H. RH (eds) *Carbonate to Clastic Facies Changes Developments in Sedimentology*. Elsevier Science Publishers, Amsterdam, pp143–174
- Berkelmans R, Weeks SJ, Steinberg CR (2010) Upwelling linked to warm summers and bleaching on the Great Barrier Reef. *Limnol Oceanogr* 55:2634–2644
- Birkeland C (1988) Geographic comparisons of coral-reef community processes. *Proceedings of the 6th International Coral Reef Symposium* 1:211–220
- Borkman DG, Smayda TJ (1998) Long-term trends in water clarity revealed by Secchi-disk measurements in lower Narragansett Bay. *ICES Journal of Marine Science* 55:668–679
- Brodie J, Wolanski E, Lewis SE, Bainbridge Z (2012) An assessment of residence times of land-sourced contaminants in the Great Barrier Reef lagoon and the implications for management and reef recovery. *Mar Pollut Bull* 65:267–279
- Brodie J, De'ath G, Devlin M, Furnas M, Wright M (2007) Spatial and temporal patterns of near-surface chlorophyll a in the Great Barrier Reef lagoon. *Marine and Freshwater Research* 58:342–353
- Brodie J, Lewis S, Bainbridge Z, Mitchell A, Waterhouse J, Kroon F (2009) Target setting for pollutant discharge management of rivers in the Great Barrier Reef catchment area. *Marine and Freshwater Research* 60:1141–1149
- Brodie J, Schroeder T, Rohde K, Faithful J, Masters B, Dekker A, Brando V, Maughan M (2010) Dispersal of suspended sediments and nutrients in the Great Barrier Reef lagoon during river-discharge events: conclusions from satellite remote sensing and concurrent flood-plume sampling. *Marine and Freshwater Research* 61:651–664
- Brodie J, Binney J, Fabricius K, Gordon I, Hoegh-Guldberg O, Hunter H, O'Reagain P, Pearson R, Quirk M, Thorburn P, Waterhouse J, Webster I, Wilkinson S (2008) Scientific Consensus Statement and the synthesis of evidence to support the Scientific Consensus Statement on water quality in the Great Barrier Reef. The State of Queensland (Department of Premier and Cabinet), Brisbane Qld 84 pp.
- Brodie JE, Devlin M, Haynes D, Waterhouse J (2011) Assessment of the eutrophication status of the Great Barrier Reef lagoon (Australia). *Biogeochemistry* 106:281–302
- Browne NK, Smithers SG, Perry CT (2010) Geomorphology and community structure of Middle Reef, central Great Barrier Reef, Australia: an inner-shelf turbid zone reef subject to episodic mortality events. *Coral Reefs* 29:683–689
- Chen Z, Muller-Karger FE, Hu C (2007) Remote sensing of water clarity in Tampa Bay. *Remote Sens Environ* 109:249–259
- Collier C, Waycott M, Ospina AG (2012) Responses of four Indo-West Pacific seagrass species to shading. *Marine Pollution Bulletin* 65 65:342–354
- Cooper TF, Uthicke S, Humphrey C, Fabricius KE (2007) Gradients in water column nutrients, sediment parameters, irradiance and coral reef development in the Whitsunday Region, central Great Barrier Reef. *Estuarine Coastal and Shelf Science* 74:458–470
- De'ath G, Fabricius K (2010) Water quality as a regional driver of coral biodiversity and macroalgae on the Great Barrier Reef. *Ecological Applications* 20:840–850
- Dennison WC (1985) The effects of light on photosynthesis and distribution of seagrasses. *Estuaries* 8:14A
- Devlin MJ, McKinna LC, Alvarez-Romero JG, Petus C, Abott B, Harkness P, Brodie J (2012) Exposure to riverine plumes in the Great Barrier Reef. Risk assessment by mapping plume extent and composition using remote sensing. *Marine Pollution Bulletin [Mar Pollut Bull]* 65:224–235

- Duarte CM (1991) Seagrass depth limits. *Aquat Bot* 40:363-377
- Eilers P, Rijnmond D, Marx B (1996) Flexible smoothing with B-splines and penalties. *Statistical Science* 11:89-121
- Fabricius K, De'ath G, Humphrey C, Zagorskis I, Schaffelke B (2013) Intra-annual variation in turbidity in response to terrestrial runoff at near-shore coral reefs of the Great Barrier Reef. *Estuarine and Coastal Shelf Science* 116:57-65
- Falkowski PG, Raven JA (1997) *Aquatic photosynthesis*. Blackwell, Malden, Mass
- Furnas MJ (2003) *Catchments and corals: terrestrial runoff to the Great Barrier Reef*. Australian Institute of Marine Science, CRC Reef. Townsville, Australia.
- Gagan MK, Chivas AR, Herczeg AL (1990) Shelf wide erosion, deposition and suspended sediment transport during cyclone Winifred, central Great Barrier Reef, Australia. *J Sediment Petrol* 60:456-470
- Hughes AO, Olley JM, Croke JC, McKergow LA (2009) Sediment source changes over the last 250 years in a dry-tropical catchment, central Queensland, Australia. *Geomorphology* 104:262-275
- Justi D, Rabalais NN, Turner RE, Dortch Q (1995) Changes in nutrient structure of river-dominated coastal waters: stoichiometric nutrient balance and its consequences. *Estuarine Coastal and Shelf Science* 40:339-356
- Kendall M, A S (1983) *The advanced theory of statistics*. Charles Griffin and Company, London
- Kirk J (1991) Volume scattering function, average cosines, and the underwater light field. *Limnology and Oceanography* [Limnol Oceanogr] 36:455-467
- Kroon FJ, Kuhnert PM, Henderson BL, Wilikinson SN, Kinsey-Henderson A, Brodie JE, Turner RDR (2012) River loads of suspended solids, nitrogen, phosphorus and herbicides delivered to the Great Barrier Reef lagoon. *Mar Pollut Bull* 65:167-181
- Lambrechts J, Hanert E, Deleersnijder E, Bernard PE, Legat V, Remacle JF, Wolanski E (2008) A multi-scale model of the hydrodynamics of the whole Great Barrier Reef. *Estuarine Coastal and Shelf Science* 79:143-151
- Lambrechts J, Humphrey C, McKinna L, Gource O, Fabricius KE, Mehta AJ, Lewis S, Wolanski E (2010) Importance of wave-induced bed liquefaction in the fine sediment budget of Cleveland Bay, Great Barrier Reef. *Estuarine Coastal and Shelf Science* 89:154-162
- Larcombe P, Woolfe K (1999) Increased sediment supply to the Great Barrier Reef will not increase sediment accumulation at most coral reefs. *Coral Reefs* 18:163-169
- Larcombe P, Ridd PV, Prytz A, Wilson B (1995) Factors controlling suspended sediment on inner-shelf coral reefs, Townsville, Australia. *Coral Reefs* 14:163-171
- Lee Z, Weidemann A, Kindlemann J, Arnone R, Carder KL, Davis C (2007) Euphotic zone depth: its derivation and implication to ocean-color remote sensing. *Geophysical Research* 112: C3
- LeGrand HM, Fabricius KE (2011) Relationship of internal macrobioeroder densities in living massive *Porites* to turbidity and chlorophyll on the Australian Great Barrier Reef. *Coral Reefs* 2011:97-107
- Lewis S, Bainbridge ZT, Kuhnert PM, Sherman BS, Henderson B, Dougall C, Cooper M, JE B (2013) Calculating sediment trapping efficiencies for reservoirs in tropical settings: a case study from the Burdekin Falls Dam, NE Australia. *Water Resources Research*
- Loya Y (1976) Effects of water turbidity and sedimentation on the community structure of Puerto Rican corals. *Bull Mar Sci* 26:450-466
- McKinnon AD, Thorrold SR (1993) Zooplankton community structure and copepod egg production in coastal waters of the Central Great Barrier Reef lagoon. *J Plankton Res* 15:1387-1411
- McQuatters-Gollop A, Gilbert AJ, Mee LD, Vermaat JE, Artioli Y, Humborg C, Wulff F (2009) How well do ecosystem indicators communicate the effects of anthropogenic eutrophication? *Estuarine and Coastal Shelf Science* 82:583-596
- Pinheiro J, Bates D (2000) *Mixed effects models in S and S-PLUS*. Springer-Verlag, New York
- Piniak GA, Storlazzi CD (2008) Diurnal variability in turbidity and coral fluorescence on a fringing reef flat: Southern Molokai, Hawaii. *Estuarine Coastal and Shelf Science* 77:56-64
- Queensland So (2013) *Reef Water Quality Protection Plan - Second Report Card*. Queensland Government
- Rogers CS (1979) The effect of shading on coral reef structure and function. *J Exp Mar Biol Ecol* 41:269-288
- Schoellhamer DH (1996) Factors affecting suspended solids concentrations in South San Francisco Bay, California. *Journal of Geophysical Research* 101 C5:12087-12095
- Schoellhamer DH (2002) Variability of suspended-sediment concentration at tidal to annual time scales in San Francisco Bay, USA. *Continental Shelf Research* 22:1857-1866

- Schroeder T, Devlin M, Brando VE, Dekker AG, Brodie J, Clementson LA, McKinna L (2012) Inter-annual variability of wet season freshwater plume extent in the Great Barrier Reef lagoon based on satellite coastal ocean colour observations. *Mar Pollut Bull* 65:210 – 223
- Smith SV, Swaney DP, Talaue-Mcmanus L, Bartley JD, Sandhei PT, McLaughlin CJ, Dupra VC, Crossland CJ, Buddemeier RW, Maxwell BA, Wulff F (2003) Humans, hydrology and the distribution of inorganic nutrient loading to the ocean. *BioScience* 53:235-245
- Smith VE, Schindler DW (2009) Eutrophication science: where do we go from here? *Trends in Ecology & Evolution [Trends Ecol Evol]* 24:201-207
- Storlazzi CD, Jaffe BE (2008) The relative contribution of processes driving variability in flow, shear, and turbidity over a fringing coral reef: West Maui, Hawaii. *Estuarine Coastal and Shelf Science* 77:549-564
- Storlazzi CD, Field ME, Bothner MH, Presto MK, Draut AE (2009) Sedimentation processes in a coral reef embayment: Hanalei Bay, Kauai. *Marine Geology* 264:140-151
- Team RDC (2013) R: A language and environment for statistical computing. R Foundation for Statistical Computing, Vienna, Austria
- The\_State\_of\_Queensland\_and\_Commonwealth\_of\_Australia (2009) Reef Water Quality Protection Plan for catchments adjacent to the Great Barrier Reef World Heritage Area. Queensland Department of Premier and Cabinet, Brisbane
- Walker TA (1981) Dependence of phytoplankton chlorophyll on bottom resuspension in Cleveland Bay, northern Queensland. *Australian Journal of Marine and Freshwater Research* 32:981–986
- Webster IT, Ford PW (2010) Delivery, deposition and redistribution of fine sediments within macrotidal Fitzroy Estuary/Keppel Bay: Southern Great Barrier Reef, Australia. *Continental Shelf Research* 30:793-805
- Weeks S, Werdell PJ, Schaffelke B, Canto M, Lee Z, Wilding JG, Feldman GC (2012) Satellite-derived photic depth on the Great Barrier Reef: Spatio-temporal patterns of water clarity. *Remote Sensing* 4:3781-3795
- Wolanski E (1994) Physical oceanographic processes of the Great Barrier Reef. CRC Press, Boca Raton
- Wolanski E, Marshall K, Spagnol S (2003) Nepheloid layer dynamics in coastal waters of the Great Barrier Reef, Australia. *J Coast Res* 19:748-752
- Wolanski E, Fabricius K, Spagnol S, Brinkman R (2005) Fine sediment budget on an inner-shelf coral-fringed island, Great Barrier Reef of Australia. *Estuarine and Coastal Shelf Science* 65:153-158
- Wood SN (2006) Generalized Additive Models: An Introduction with R. Chapman and Hall/CRC Press
- Wood SN (2011) Fast stable restricted maximum likelihood and marginal likelihood estimation of semiparametric generalized linear models. *Journal of the Royal Statistical Society Series B* 73:3-36